Elevation Angular Dependence of Wideband Autocorrelation Radiometric (WiBAR) Remote Sensing of Dry Snowpack and Lake Icepack

SEYEDMOHAMMAD MOUSAVI[1], ROGER DE ROO[2], KAMAL SARABANDI[1], AND ANTHONY W. ENGLAND[3]

ABSTRACT

A novel and recently developed microwave radiometric technique, known as wideband autocorrelation radiometry (WiBAR), offers a deterministic method to remotely sense the microwave propagation time $\boldsymbol{\tau_{delay}}$ of multi-path microwave emission of low loss terrain covers and other layered surfaces such as dry snowpack and freshwater lake icepack. The microwave propagation time $\boldsymbol{\tau_{delay}}$ through the pack yields a measure of its vertical extent; thus, this technique is a direct measurement of depth. We have confirmed the expected simple dependence of the microwave propagation time $\boldsymbol{\tau_{delay}}$ on the elevation angle with ground-based WiBAR measurements of the icepack on Douglas Lake in Michigan in early March 2016. The observations are done in the X-band for the icepack. At these frequencies, the volume and surface scattering are small in the pack. This technique is inherently low-power since there is no transmitter as opposed to active remote sensing techniques. In this paper, the system design parameters and physics of operation of the WiBAR is discussed, and it is shown that the microwave propagation time can be readily MEASURED FOR dry snowpack and lake icepack for observation angles away from nadir to at least 70°.

Keywords: Snowpack, icepack, remote sensing, microwave radiometry

INTRODUCTION

With the rapid industrial and human population growth, the demand for accurate remote sensing instruments and techniques for monitoring the environmental changes and management of natural sources is increasing. Environmental changes such as climate warming impose rapid changes upon the cryosphere (Serreze, Walsh, Chapin, Zhang, & Barry, 2000); as a result, the statistics which demonstrate the extent, timing, and snow water equivalent (SWE) of seasonal snowpacks on prairie and alpine terrains are no longer stationary (Milly, et al., Feb. 2008). Effective management of the freshwater reservoir requires almost daily monitoring the spatial and temporal distribution of SWE and snowpack wetness. Such tasks are appropriate for satellite sensors or sensors on long duration solar powered autonomous airborne vehicles which are weakly served by current technologies.

[1] Electrical Engineering and Computer Science Department, University of Michigan, Ann Arbor, MI.

[2] Climate and Space Sciences and Engineering Department, University of Michigan, Ann Arbor, MI.

[3] College of Engineering and Computer Science, University of Michigan, Dearborn, MI.

Due to their all-weather operation capability, both microwave radar and radiometer systems have long been proposed and implemented as powerful remote sensing tools in retrieving the physical parameters of interest. For most remote sensing applications, the gross parameters of the target, such as vertical extent of snowpack/icepack and SWE, are often the parameters of interest. Current microwave remote sensing of dry snowpack is based on frequency-dependent differential scattering by the ice grains that comprise snowpacks, referred to as scatter darkening. In the case of microwave radiometry, this phenomenon was first recognized as contributing to the microwave brightness of snowpacks, sea ice, frozen soils, and planetary regolith (England, Apr. 1974), (England, Thermal microwave emission from a scattering layer, Nov. 1975). Scatter darkening has been developed as a SWE remote sensing technology over the last three decades (Chang, Foster, Hall, Rango, & Hartline, 1982), (Hallikainen, Jan. 1992), (Koike & Suhama, 1993). Scatter darkening affects the microwave brightness temperature of media such as snowpacks. At higher frequencies (shorter wavelengths), upwelling microwave radiation experiences greater scattering; thus, the spectral gradient of microwave brightness temperature becomes significantly more negative as the snow on the ground accumulates. For example, differences between microwave brightness temperatures at two different frequencies, namely 19 and 37 GHz, are used in an empirical algorithm by Environment Canada to estimate the SWE of snowpacks on the Canadian Great Plains reported on CCIN URL (https://www.ccin.ca/home/ccw/snow/current).

Scatter darkening based microwave radiometry for estimating the layer thickness is not robust since the scattering theory yields only the form of frequency dependent scatter darkening but not a reliable amplitude estimation. The algorithm should be empirically tuned to a region's typical snowpack. Thus, it is highly dependent on the microscopic properties of the snowpack (e.g. grain size), which varies considerably from place to place and time to time. For example, non-seasonably warm weather and early and late season diurnal heating cause metamorphic growth of the ice grains in the snowpacks, which turns into a greater scatter darkening. In addition, tuning algorithms become very complicated or even unworkable for terrains that are more complex than the Canadian Great Plains. In the search for an alternative and more effective approach, the application of wideband autocorrelation radiometry (WiBAR) for retrieving the physical parameters of low loss terrestrial targets is investigated in this paper. As will be shown, the vertical extent of the dry snowpack or lake icepack can be directly measured for different observation angles away from nadir by sensing the microwave propagation time through the pack.

WIDEBAND AUTOCORRELATION RADIOMETRY (WIBAR)

Wideband autocorrelation radiometry (WiBAR), offers a deterministic method to remotely sense the propagation time $\boldsymbol{\tau_{delay}}$ of multi-path microwave emission of low-loss terrain covers and other layered surfaces. Terrestrial examples are the snow and lake ice packs. This technique makes use of the correlation that exists between the thermal radiation from the surface beneath or within the pack which travels upwards through the pack towards the radiometer, which will be referred to as the direct signal, and other portion of the radiation that reflects back from the pack's upper interface then from its lower interface, before traveling towards the radiometer's antenna, as shown in

Figure 1. Thus, there are two signals received by the radiometer, the direct signal and a delayed copy of it. The delayed signal arrives at the radiometer with the time delay $\boldsymbol{\tau_{delay}}$, where (England, Apr. 2013)

$$\begin{aligned} \boldsymbol{\tau_{delay}} &= \boldsymbol{2\tau_p - \tau_{air}} \\ \boldsymbol{\tau_{air}} &= \frac{\boldsymbol{2d\ \tan\theta_p\ \sin\theta_{air}}}{\boldsymbol{c}} \\ \boldsymbol{\tau_p} &= \left(\frac{\boldsymbol{d}}{\boldsymbol{\cos\theta_p}}\right)\left(\frac{\boldsymbol{n_p}}{\boldsymbol{c}}\right) \end{aligned} \quad (1)$$

τ_p is the one way travel time in the pack, τ_{air} is the travel time in the air between points P_1 and P_2, n_p is the refractive index of the pack, and c is the speed of light in free space. The microwave

propagation time τ_{delay} through the pack yields a measure of it vertical extent. Incidence angles θ_p and θ_{air} are related by Snell's law.

$$\boldsymbol{n_p \sin \theta_p = \sin \theta_{air}} \quad (2)$$

An estimate of n_p for the dry snowpack can be obtained by the empirical relationships (Ulaby, Moore, & A. K. Fung, 1986)

$$\begin{aligned} \boldsymbol{n_s} &= \sqrt{\boldsymbol{1.0 + 1.9\rho_s}} && \boldsymbol{\rho_s \leq 0.5}\ \text{g.cm}^{-3} \\ &= \sqrt{\boldsymbol{1.0 + 1.9\rho_s}} && \boldsymbol{\rho_s \geq 0.5}\ \text{g.cm}^{-3} \end{aligned} \quad (3)$$

ρ_s is the density of dry snowpack, and is related to the snow water equivalent (SWE) and the snow depth (d) by

$$\text{SWE} = \left(\frac{\boldsymbol{\rho_s}}{\boldsymbol{\rho_\omega}}\right)\boldsymbol{d} \quad (4)$$

Where the freezing point density of water is $\rho_\omega = 1.00\ \text{g/cm}^3$.

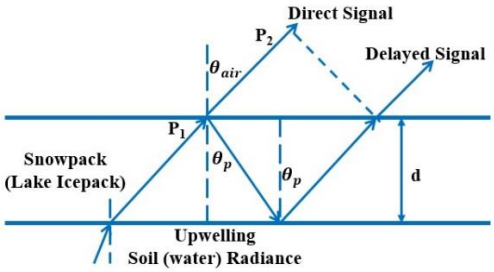

Figure 1. Remote sensing of microwave travel time within the pack using Wideband Autocorrelation Radiometry (WiBAR). The direct signal and the delayed signal arrive at the radiometer antenna with the time difference $\boldsymbol{\tau_{delay}}$.

On other hand, the refractive index of the pure icepack is an almost constant value of $\sqrt{3.15}$ (Evans, 1965). It should be noted that the wetness in the pack will introduce an attenuation in the signal propagating through the pack since the refractive index is complex in this scenario. However, exploring this potential is beyond the scope of this paper, and the focus in here is sensing the microwave propagation time in dry snowpacks/icepacks.

MODELING OF DRY SNOWPACK AND LAKE ICEPACK

A layered medium with boundaries at $z = -d_0, -d_1, \ldots, -d_N$ with $d_0 = 0$ is shown in Figure 2. It is assumed that the top (region 0) and the bottom (region N+1) layers are semi-infinite. It is assumed that the temperature profile of the layers is uniform, the layers are homogeneous, and the interfaces between the layers are electrically smooth. Hence, the Fresnel reflection coefficients can be used in order to obtain the reflectivity and emissivity of the layered medium. The plane of incidence is determined by the z-axis and the incident $\bar{k}$ vector. The horizontally polarized (TE) configuration is discussed in this section since the outdoor measurements were conducted with horizontally polarized (TE) configuration. However, the solutions for the vertically polarized (TM) configuration can be readily obtained using the duality relationships $\bar{E} \to \bar{H}, \bar{H} \to -\bar{E}, \mu \leftrightarrow \epsilon$.

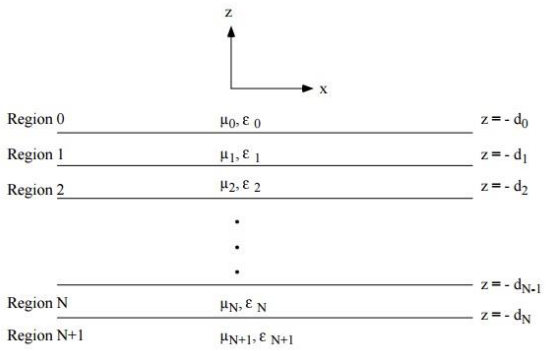

Figure 2. Configuration of N+1 layered medium.

For a horizontally polarized (TE) incident wave, the reflection coefficient in region l at the interface separating regions l and l+1 is given by

$$\boldsymbol{R_{l(l+1)}} = \frac{\mu_{l+1}k_{lz} - \mu_l k_{(l+1)z}}{\mu_{l+1}k_{lz} + \mu_l k_{(l+1)z}} \tag{5}$$

where A_l and B_l are the coefficients of the upward and downward going wave in region l, respectively. In addition, k_{lz} is the propagation constant along the z-axis in each region l. By forcing the boundary condition at each interface, it can be shown that (Tsang, Kong, & R. T. Shin, 1985)

$$\frac{A_l}{B_l} e^{-i2k_{lz}d_l} = \frac{\frac{A_{l+1}}{B_{l+1}} e^{-i2k_{(l+1)z}d_{l+1}} e^{i2k_{(l+1)z}(d_{l+1}-d_l)} + R_{l(l+1)}}{\frac{A_{l+1}}{B_{l+1}} e^{-i2k_{(l+1)z}d_{l+1}} R_{l(l+1)} e^{i2k_{(l+1)z}(d_{l+1}-d_l)} + 1} \tag{6}$$

This is a recurrence relation which can be used to find $R_h = A_0/B_0$ starting from $A_{N+1}/B_{N+1} = 0$, since there is no upward going wave ($A_{N+1} = 0$) in the semi-infinite region N+1. The emissivity e can now be obtained from the reflectivity r by

$$\boldsymbol{e = 1 - r} \tag{7}$$

and the reflectivity is given by

$$\mathbf{r} = |\mathbf{R}|^2 \tag{8}$$

where R is the reflection coefficient of the layered medium in either horizontally (TE) or vertically (TM) polarized configuration.

For the case of a lake icepack without a snowpack on top over freshwater or a snowpack over soil, the configuration is shown in Figure 3. Using the recurrence relation (6), the reflection coefficient of this medium is given by

$$\boldsymbol{R} = \frac{\boldsymbol{R_{01}+R_{12}e^{i2k_{1z}d_1}}}{\boldsymbol{1+R_{01}R_{21}e^{i2k_{1z}d_1}}} \tag{9}$$

R_{01} and R_{12} are the Fresnel reflection coefficients at the air-snow/ice and snow/ice-soil/freshwater interfaces, respectively, and is given by the equation (5). Using the equation (7), the emissivity can be obtained as follow

$$\boldsymbol{e} = \frac{\boldsymbol{(1-|R_{01}|^2)(1-|R_{12}|^2)}}{\boldsymbol{1+(|R_{01}||R_{12}|)^2+2|R_{01}||R_{12}|\cos(2k_{1z}d_1)}} \tag{10}$$

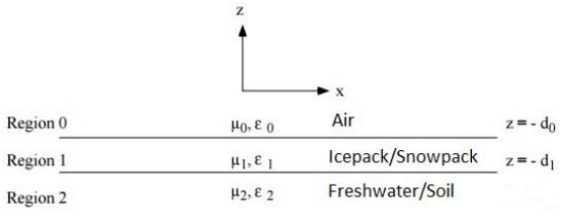

Figure 3. Configuration of the lake icepack without a snowpack on top over freshwater or a snowpack over soil.

On the other hand, for the case of a lake icepack with a snowpack on top over freshwater, the configuration is as shown in Figure 4. Using the recurrence relation (6), the reflection coefficient of this medium is given by

$$\boldsymbol{R} = \frac{\boldsymbol{R_{01}+\left[\frac{R_{12}+R_{23}e^{i2k_{2z}(d_2-d_1)}}{1+R_{23}R_{12}e^{i2k_{2z}(d_2-d_1)}}\right]e^{i2k_{1z}d_1}}}{\boldsymbol{1+\left[\frac{R_{12}+R_{23}e^{i2k_{2z}(d_2-d_1)}}{1+R_{23}R_{12}e^{i2k_{2z}(d_2-d_1)}}\right]R_{01}e^{i2k_{1z}d_1}}} \tag{11}$$

In this equation R_{12} and R_{23} are the reflection coefficients at the snow-ice and ice-freshwater interfaces, respectively. In addition, R_{01} is the reflection coefficient at the air-snow interface. Similarly, the emissivity of this medium is given by

$$\boldsymbol{e} = \frac{\boldsymbol{(1-|R_{01}|^2)(1-|R_{12}|^2)(1-|R_{23}|^2)}}{\boldsymbol{\gamma+\chi+\alpha+\beta}}$$

$$\boldsymbol{\gamma = 1 + |R_{01}|^2\,|R_{12}|^2 + |R_{01}|^2\,|R_{23}|^2 + |R_{12}|^2\,|R_{23}|^2}$$

$$\chi = 2\,|R_{12}||R_{23}|(1+|R_{01}|^2)\cos(2k_{2z}(d_2-d_1)) + 2\,|R_{01}||R_{12}|(1+|R_{23}|^2)\cos(2k_{1z}d_1)$$
$$\alpha = 2\,|R_{01}||R_{23}|\cos[2(k_{2z}(d_2-d_1)+k_{1z}d_1)]$$
$$\boldsymbol{\beta = 2\,|R_{01}||R_{23}||R_{12}|^2\cos[2(k_{2z}(d_2-d_1)-k_{1z}d_1)]} \tag{12}$$

It can be observed from equation (12) that time delays proportional to the summation and difference of the layer thicknesses have also been introduced.

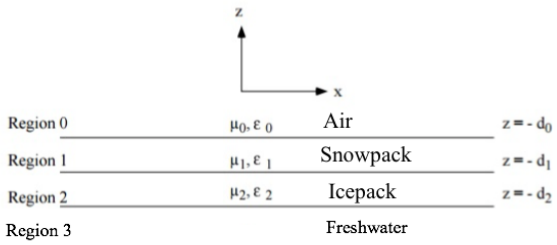

Figure 4. Configuration of the lake icepack with a snowpack on top over freshwater.

Since the cosine terms in equations (10) and (12) are in the denominator of these equations, and they are responsible for the microwave propagation time through the packs, it would be better to work with the inverse of the emissivity (1/e) in order to obtain the autocorrelation response. The autocorrelation response of an icepack with thickness $d_{ice} = d_1 - d_2 = 36.83$ cm and without a snowpack is shown in Figure 5. The observation angle is at nadir ($\theta_0 = 0$). The autocorrelation response of the inverse of the emissivity for the icepack with and without snowpack on top is also plotted in Figure 6. The icepack thickness is $d_{ice} = 36.83$ cm, and the snowpack thickness is $\$d_{snow} = d_1 = 3.98$ cm. The observation angle is again at nadir ($\theta_0 = 0$). It can be observed that new peaks appear in the case of icepack with snowpack on top.

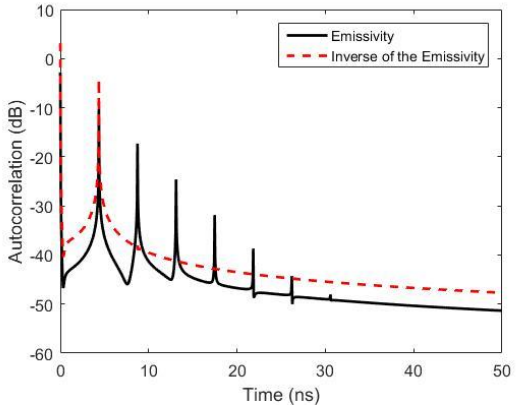

Figure 5. Autocorrelation response of the emissivity and its inverse for an icepack without a snowpack on top ($\boldsymbol{\theta_0 = 0}$ and $\boldsymbol{d_{ice} = 36.83}$ cm).

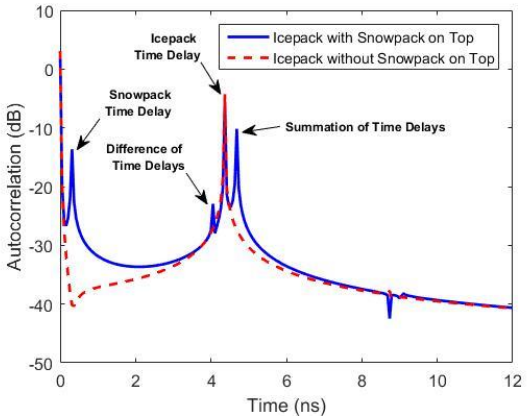

Figure 6. Autocorrelation response of the inverse of the emissivity for an icepack without a snowpack on top ($\boldsymbol{\theta_0 = 0}$, $\boldsymbol{d_{ice} = 36.83}$ cm, and $\boldsymbol{d_{snow} = 3.98}$ cm).

EXPERIMENTAL MEASUREMENTS AND RESULTS

In the previous section, the expressions for the emissivity of lake icepack with and without snowpack on top were derived. It was shown theoretically that the WiBAR technique can directly measure the thickness of the low loss layers. The objective of this section is to demonstrate the potential of the WiBAR technique as an inversion algorithm. Experimental measurements for lake icepack were conducted over Douglas Lake at the University of Michigan Biological station (UMBS) on March, 2016. The operation frequency range was 7-10 GHz. The measurement were conducted at observation angles away from nadir up to at least 70^O. A motorcycle battery was used as a power source for the low noise amplifier of the receiver gain chain, as shown in Figure 7. The receiver gain chain of the WiBAR after the antenna includes an isolator, a low noise amplifier (LNA), a band-pass filter (BPF), another LNA, and finally another isolator before getting connected to the spectrum analyzer (SA). The schematic of the reciver gain chain is shown in Figure 8. Using the ground truth measurements, the icepack thickness was found to be 14.5 inches ($d_{ice} = 36.83$ cm), and the snowpack on top of the icepack was found to be $d_{snow} = 3.98$ cm, as shown in Figure 9.

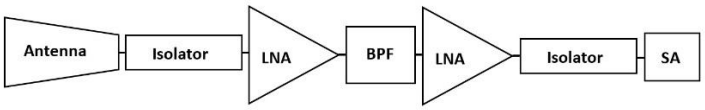

Figure 7. The schematic of the receiver gain chain of the WiBAR radiometer.

Figure 8. Measurement setup of the lake icepack measurement using a wideband autocorrelation radiometer.

Figure 9. Ground truth measurements of the lake icepack and the snowpack on top ($\boldsymbol{d_{ice} = 36.83}$ cm, and $\boldsymbol{d_{snow} = 3.98}$ cm).

Measurements of sky and microwave absorber were also measured to obtain spectra for targets whose emissivity approximated 0 and 1, respectively. These were then used to correct the averaged power spectra of the target to yield spectra of emissivity. As an example, one of the power spectrum of the sky, absorber, and lake ice observations on Douglas Lake on March 02, 2016 are shown in Figure 10. To find the time delay, the reciprocals of the emissivity spectra were multiplied by a Blackman window, zero-padded to improve temporal resolution, and inverse Fourier transformed to yield an autocorrelation function. As an example, the emissivity and the autocorrelation function of the same observation are shown in Figure 11 and Figure 12, respectively.

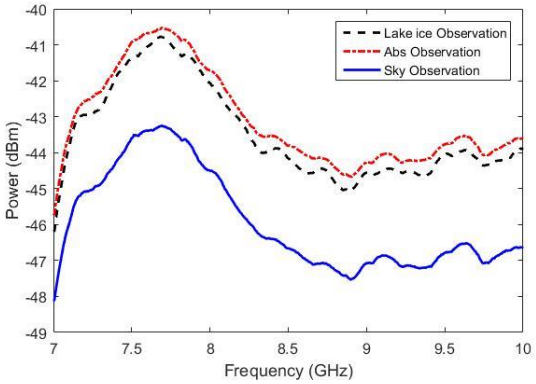

Figure 10. Sky, load, and lake icepack observations on Douglas Lake on March 02, 2016.

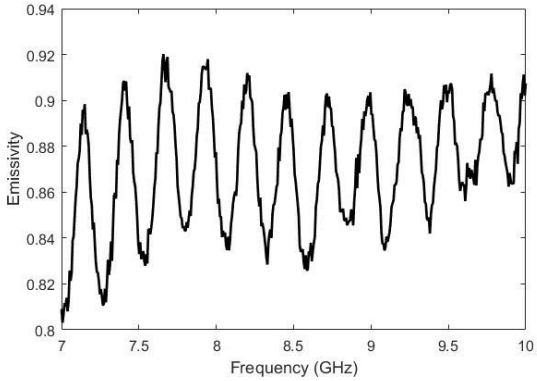

Figure 11. The emissivity of the lake icepack measured on Douglas Lake on March 02, 2016.

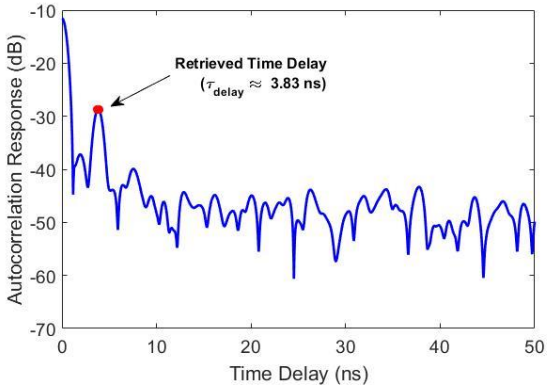

Figure 12. The autocorrelation response of the lake icepack measured on Douglas Lake on March 02, 2016.

The retrieved microwave propagation times for the icepack without and with snowpack on top of it with respect to observation angle is plotted in Figure 13 and Figure 14, respectively. The expected values for the microwave propagation time through the icepack are obtained using the equation (1). It can be observed that there is a good fit between the estimated and expected values.

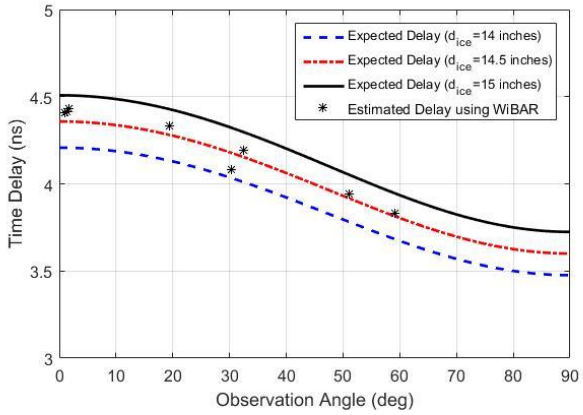

Figure 13. Estimated and expected microwave propagation time through the icepack without snowpack on top with respect to the observation angle ($\boldsymbol{d_{ice} = 36.83}$ cm).

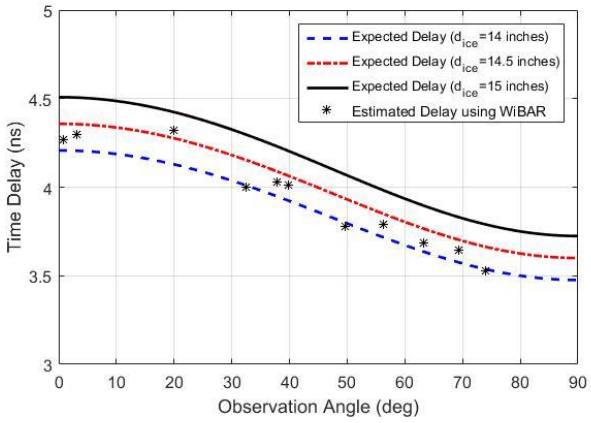

Figure 14. Estimated and expected microwave propagation time through the icepack with snowpack on top with respect to the observation angle ($\boldsymbol{d_{ice} = 36.83}$ cm, and $\boldsymbol{d_{snow} = 3.98}$ cm).

CONCLUSIONS

The potential of the WiBAR technique as a useful remote sensing tool was demonstrated in this paper. Analytical expressions for the emissivity of an icepack with and without a snowpack on top it were derived. It was shown that the WiBAR can directly measure the dry snowpack or lake icepack vertical extent. Thus, it is a deterministic method of remotely sensing the snowpack SWE, wetness, and sub-pixel SWE variance. Experiments were conducted using the wideband autocorrelation radiometer at X-band for the lake icepack with and without snowpack on top of it in order to demonstrate the feasibility of the target parameter retrieval. The success of this technique was demonstrated by comparing the estimated time delayed with expected time delays obtained from ground truth measurements.

REFERENCES

Chang AT, Foster JL, Hall DK, Rango A, Hartline BK. 1982. Snow water equivalent estimation by microwave radiometry. *Cold Regions Science and Technology* **5**: 259-267.

England AW. 1974. Thermal microwave emission from a halfspace containing scatterers. *Radio Science* **9**: 447-454.

England AW. 2013. Wideband autocorrelation radiometric sensing of microwave travel time in snowpacks and planetary ice layers. *IEEE Transactions on Geoscience and Remote Sensing* **51**: 2316-2326.

England AW. 1975. Thermal microwave emission from a scattering layer. *Journal of Geophysical Research* **80**: 4484-4496.

Evans S. 1965. Dielectric properties of ice and snow. *Journal of Glaciology* **5**: 773-792.

Hallikainen MT, Jolma PA. 1992. Comparison of algorithms for retrieval of snow water equivalent from Nimbus-7 SMMR data in Finland. *IEEE Transactions on Geoscience and Remote Sensing* **30**: 124-131.

Koike T, Suhama T. 1993. Passive-microwave remote sensing of snow. *Annals of Glaciology* **18**: 305-308.

Milly PC, Beancourt J, Falkenmark M, Hirsch RM, Kundzewiez W, Lettenmaier DP, Stouffer RJ. 2008. Stationary is dead: Whither water management? *Science* **319**: 573-574.

Serreze MC, Walsh JE, Chapin IF, Zhang T, Barry RG. 2000. Observational evidence of recent change in the northern high-latitude environment. *Climatic Change* **46**: 159-207.

Tsang L, Kong JA, Shin RT. 1985. *Theory of Microwave Remote Sensing.* New York: John Wiley and Sons.
Ulaby FT, Moore RK, Fung AK. 1986. *Microwave Remote Sensing: Active and Passive, Vol III.* Norwood, MA: Artech House.